HHS Public Access

Author manuscript

Neurobiol Dis. Author manuscript; available in PMC 2022 June 15.

Published in final edited form as:

Neurobiol Dis. 2022 June 15; 168: 105712. doi:10.1016/j.nbd.2022.105712.

Methamphetamine augments HIV-1 gp120 inhibition of synaptic transmission and plasticity in rat hippocampal slices: Implications for methamphetamine exacerbation of HIV-associated neurocognitive disorders

Ya Zheng[1], **Benjamin Reiner**[2], **Jianuo Liu**, **Linda Xu**, **Huangui Xiong**[*]

The Neurophysiology Laboratory, Department of Pharmacology and Experimental Neuroscience, University of Nebraska Medical Center, Omaha, NE 68198-5880, USA

Abstract

Methamphetamine (Meth) abuse and human immunodeficiency virus type 1 (HIV-1) infection are two major public health problems worldwide. Being frequently comorbid with HIV-1 infection, Meth abuse exacerbates neurocognitive impairment in HIV-1-infected individuals even in the era of combined antiretroviral therapy. While a large body of research have studied the individual effects of Meth and HIV-1 envelope glycoprotein 120 (gp120) in the brain, far less has focused on their synergistic influence. Moreover, it is well-documented that the hippocampus is the primary site of spatial learning and long-term memory formation. Dysregulation of activity-dependent synaptic transmission and plasticity in the hippocampus is believed to impair neurocognitive function. To uncover the underlying mechanisms for increased incidence and severity of HIV-1-associated neurocognitive disorders (HAND) in HIV-1-infected patients with Meth abuse, we investigated acute individual and combined effects of Meth (20 μM) and gp120 (200 pM) on synaptic transmission and plasticity in the CA1 region of young adult male rat hippocampus, a brain region known to be vulnerable to HIV-1 infection. Our results showed that acute localized application of Meth and gp120 each alone onto the CA1 region reduced short-term dynamics of input-output responses and frequency facilitation, and attenuated long-term potentiation

[*]Corresponding author: hxiong@unmc.edu (H. Xiong).

[1]Present address: Department of Rehabilitation Medicine, Tongji Hospital Affiliated to Tongji University School of Medicine, Shanghai 200,065, China.

[2]Present address: Molecular and Neural Basis of Psychiatric Disease Section, Department of Psychiatry, University of Pennsylvania Perelman School of Medicine, Philadelphia, PA 19104

Author contributions

H.X. directed study; Y.Z., H.X analyzed, interpreted results, and wrote the manuscript; Y.Z., B.R., J. L., L.X. performed experiments and collected/analyzed data; All authors read and approved the manuscript.

Ethics approval and consent to participate

All experimental protocols and animal care were carried out in accordance with the National Institutes of Health *Guide for the Care of Laboratory Animals in Research* and approved by the Institutional Animal Care and Use Committee of the University of Nebraska Medical Center (IACUC # 19-085-07-FC).

CRediT authorship contribution statement

Ya Zheng: Investigation, Visualization, Writing – original draft, Writing – review & editing. **Benjamin Reiner:** Investigation, Writing – original draft. **Jianuo Liu:** Conceptualization, Investigation, Validation. **Linda Xu:** Investigation, Validation. **Huangui Xiong:** Conceptualization, Supervision, Writing – review & editing, Funding acquisition.

Declaration of Competing Interest

The authors declare that they have no competing of interests.

(LTP) induced by either high frequency stimulation or theta burst stimulation. A synergistic augmentation on activity-dependent synaptic plasticity was observed when Meth and gp120 were applied in combination. Paired-pulse facilitation results exhibited an altered facilitation ratio, suggesting a presynaptic site of action. Further studies revealed an involvement of microglia NLRP3 inflammasome activation in Meth augmentation of gp120-mediated attenuation of LTP. Taken together, our results demonstrated Meth augmented gp120 attenuation of LTP in the hippocampus. Since LTP is the accepted experimental analog of learning at the synaptic level, such augmentation may underlie Meth exacerbation of HAND observed clinically.

Keywords

Methamphetamine; HIV-1gp120; Hippocampal slices; Synaptic transmission; Long-term potentiation; Microglia; Inflammasome

1. Introduction

Human immunodeficiency virus type 1 (HIV-1) brain infection often provokes cognitive and behavior deficits collectively termed as HIV-1-associated neurocognitive disorders (HAND) (Antinori et al., 2007; Saylor et al., 2016) which was characterized by severe cognitive dysfunction and mortality in the pre-antiretroviral era (Antinori et al., 2007; Navia et al., 1986). The implementation of combined antiretroviral therapy (cART) has led to a sharp decline in the mortality attributed to AIDS and dramatically reduced incidence of severe form of HAND in infected individuals (Heaton et al., 2011; Saylor et al., 2016). The widespread of cART has also transformed the HIV-1 infection from a life-threatening illness to a manageable chronic disease (Heaton et al., 2011). Nevertheless, in the cART era, viral persistence in brain in a latent or restrict manner continues to play a significant disease-inciting role. Whilst the most severe form of HAND is now rare, milder forms of cognitive impairment persist among people living with HIV-1 and prevalence of these forms of cognitive impairment is in fact on the rise (Heaton et al., 2011; Saylor et al., 2016). Although the underlying mechanisms remain obscure, several risk factors have been identified including, but are not limited to, HIV-1 envelope glycoprotein 120 (gp120)-induced neurotoxicity (Kesby et al., 2015b; Sanchez et al., 2015) and comorbid drug abuse, in particular, the psychostimulant methamphetamine (Meth) (Lanman et al., 2021; Sanchez and Kaul, 2017).

The viral protein gp120 has been identified as a potent neurotoxin involved in the HAND pathogenesis with deleterious effects at concentrations ranging from picromolar to nanomolar in vitro (Klasse and Moore, 2004; Oh, 1992), or higher (Cummins et al., 2010). Such potency might be reflexive of its biological relevance in vivo (Gilbert et al., 2003). Indeed, soluble gp120 at high concentrations has been detected in the peripheral blood and secondary lymphoid organs of individuals with chronic HIV infection (Santosuosso et al., 2009), in addition to anti-gp120 antibodies in cerebral spinal fluid of patients with HAND (Trujillo et al., 1996). Studies have shown that gp120, shed off from HIV-1 virions and/or released from infected brain cells (Saylor et al., 2016; Smith et al., 2018), on the one hand, induces neuronal apoptosis, synaptic and dendrite dysfunction (McIntosh et al., 2015;

Timilsina and Gaur, 2016); and, on the other hand, causes immune activation and resultant production of neurotoxic molecules as well as inflammasome-dependent pyroptosis (He et al., 2020) leading to the development of HAND (Smith et al., 2018). The neurocognitive impairment and pathophysiological alterations observed in HIV-1-infected individuals can be attributed to direct and indirect effects of gp120 and are frequently associated with the use of psychostimulant drugs such as Meth (Chilunda et al., 2019; Kapadia et al., 2005).

Meth is one of the most common abused drugs among individuals infected with HIV-1 (Marquez et al., 2009). Accumulating evidence indicates that Meth abuse not only increases the risk of HIV-1 infection (Gonzales et al., 2010; Mitchell et al., 2006), but also exacerbates the cognitive deficits and neurodegenerative abnormalities in HIV-1-infected patients as well as in gp120 transgenic (gp120-tg) animals (Henry et al., 2013; Hoefer et al., 2015; Kesby et al., 2015a; Thaney et al., 2018). It has shown that HIV-1 infection and Meth abuse each alone may cause neuronal injury and cognitive impairment (Larsen et al., 2002; Mattson et al., 2005). In contrast, they in combination appear to produce more serious neurocognitive impairment than each alone. Indeed, Meth was found to exacerbate HAND in HIV-1-infected individuals (Chana et al., 2006; Silverstein et al., 2012). However, the mechanisms underlying Meth exacerbation of HIV-/gp120-associated cognitive impairment are incompletely understood.

The hippocampus is one of the most thoroughly investigated brain structure widely believed to be involved in learning and memory (Bird and Burgess, 2008; Knierim, 2015). Increasing evidence indicate that impairment of hippocampal structure and function occurs in HIV-1-infected individuals and Meth abusers, which is associated with cognitive deficits (Castelo et al., 2006; Kelschenbach et al., 2019; Thompson et al., 2004). It has been shown that Meth abuse could result in increase of Nod-like Receptor Protein 3 (NLRP3) inflammasome activation in the hippocampal region of postmortem Meth chronic user (Mahmoudiasl et al., 2019) and NLRP3 inflammasome activation is involved in Meth- and gp120-associated neurotoxic activities (Du et al., 2019; He et al., 2020; Walsh et al., 2014; Xu et al., 2018). To understand how Meth exacerbates HIV-1-associated neurocognitive impairment, we studied the acute effects of Meth and gp120 on synaptic transmission and plasticity in rat hippocampal brain slices. Our results showed that Meth and gp120 each alone had an inhibitory effect on short- and long-term synaptic plasticity in the CA1 region, and this inhibition was augmented when Meth and gp120 tested in combination. Further studies revealed a presynaptic site of action and involvement of microglia NLRP3 inflammasome activation in Meth- and gp120-mediated inhibition of synaptic activity.

2. Materials and methods

2.1. Materials

Full-length HIV-1_{MN} gp120 (gp120, Clade B) was purchased from Immunodiagnostics, Inc. (Woburn, MA). Aliquots of gp120 were kept as 100 nM stock solution at −80 °C. The stock solution was diluted to desired concentrations with artificial cerebrospinal fluid (ACSF) 2–5 min before test. Methamphetamine was purchased from Sigma-Aldrich (St. Louis, MO, Cat # M-8750) with DEA license # RX0374974. Lipopolysaccharide (LPS, from *Escherichia coli* 0111:B4) was also purchased Sigma-Aldrich. Ac-YVAD-CMK was obtained from Enzo

Life Sciences (Farmingdale, NY). All other chemicals, unless otherwise specified, were purchased from Sigma-Aldrich.

2.2. Animals

Male Sprague-Dawley rats (16- to 31-day-old) used for this study were purchased from Charles River Laboratories (Wilmington, MA). Animals were housed at constant temperature (22 °C) and relative humidity (50%) under a regular light-dark cycle (light on at 7 am and off at 5 pm) with free access to food and water. All animal use procedures were strictly reviewed by the Institutional Animal Care and Use Committee (IACUC) of University of Nebraska Medical Center (IACUC No. 19–085-07-FC).

2.3. Hippocampal slices

Rat hippocampal brain slices were prepared as previously described (Xiong et al., 1996). Briefly, animals were anesthetized with isoflurane, decapitated, and their brains were quickly removed from the cranial cavity. The brains were placed into an ice-cold (4 °C) oxygenated artificial cerebrospinal fluid (ACSF) environment. The hippocampi were dissected free and transverse hippocampal slices (400 μm in thickness) were cut using a tissue chopper. The slices were kept in a humidified/oxygenated interface chamber at room temperature (22 °C) for at least 1 h before being transferred into a recording chamber. In the recording chamber, a single hippocampal slice, rested on a nylon mesh ring sat closely to the bottom of the chamber fully, was submerged in a continuously perfused ACSF solution at a constant flow rate of 2 ml/min with the use of a peristaltic pump (Rainin Instrument Co., Woburn, MA). The ACSF contained (in mM): NaCl (124.0), KCl (3.0), $CaCl_2$ (2.0), $MgCl_2$ (2.0), NaH_2PO_4 (1.25), $NaHCO_3$ (26.0) and Glucose (10.0), equilibrated with 95% O_2 and 5% CO_2, had a pH of 7.4–7.5 and an osmolarity of ~305 mOsm. The temperature of the perfusion was maintained at 30 ± 1 °C with an automatic temperature controller (Warner Instrument Corp., Hamden, CT). Biological reagents were applied onto the slices and incubated in humidified/oxygenated interface chamber for 1 h prior to conducting electrophysiology recordings. Experimental timeline is shown in Fig. 1.

2.4. Electrophysiology

Field excitatory post-synaptic potentials (fEPSPs) were generated by test pulses applied every 20s (low frequency) with a constant current (100–300 μA, 40 μs in duration) stimulation of Schaffer collateral-commissural axons using an insulated bipolar tungsten electrode. The stimulation intensity was adjusted to generate approximately 40–50% of a maximal response. The evoked fEPSPs were recorded with an Axopatch-1D amplifier (Molecular Devices, San Jose, CA) in the CA1 dendrite field and Clampex 10 (Molecular Devices) was used for data acquisition. The recording microelectrodes were made from borosilicate glass capillaries (WPI, Sarasota, FL) with inner filaments that enable quick back-filling with ACSF (resistance of 1–5 MΩ). Electrical signals were filtered at 1.0 kHz and digitized at 5.0 kHz using a Digidata 1440 interface (Molecular Devices). Data were stored on a desktop PC and analyzed off-line using pCLAMP 10 software (Molecular Devices) and OriginPro 2019b (OriginLab, Northampton, MA). To eliminate the possibility that gp120 and Meth activate inhibitory interneurons, a portion of early experiments were conducted in the presence of 20 μM picrotoxin, except those testing the effects of Meth/

gp120 on basal synaptic transmission. To prevent epileptiform activities, a surgical cut was made between CA1 and CA3 areas after the slice had been transferred to the recording chamber.

For LTP experiment, a 30 min-baseline recording was conducted once the adjustment of stimulation parameters was achieved. High frequency stimulation (HFS, 100 Hz, 500 ms/train × 3) was delivered 30 min after the start of recording on each slice with an inter-train interval of 20 s. Each recording trial was an average of 3 consecutive sweeps. The initial slope of fEPSP was analyzed and expressed in percentage of basal level, i.e., the average of initial slopes from the first 30 min in HFS and 15 min in theta-burst stimulation (TBS) were treated as 100%, respectively. In bar graphs, the magnitudes of LTP were quantified as the average of entire 60 min recordings after HFS and entire 45 min recordings after TBS. All data were expressed as the mean ± standard error of the mean (SEM) unless otherwise indicated. To mimic physiological condition, the TBS was also employed to induce LTP (TBS-LTP). The TBS protocol, as described previously (Morgan and Teyler, 2001), was composed of 5 trains of 4 pulses (100 Hz) at a rate of 1 train per 200 ms and repeated twice with an interval of 10 s. Like in HFS-LTP, a baseline recording was conducted for 15 min before TBS stimulation. Changes in LTP were evaluated with the same method as HFS-LTP.

Input-output (I–O) tests were conducted by setting the stimulus intensity to evoke 40–50% of maximal fEPSPs. The stimulus intensities were from 0.2 mA to 0.8 mA with an increment of 0.1 mA and resultant fEPSPs were recorded and analyzed. Paired pulse ratio (PPR) curves were generated by testing the Schaffer-collateral pathway with twin pulses at a fixed pulse duration of 40 μs with varying inter-pulse interval (IPI) at a 20 ms increment from 20 ms to 100 ms. The paired pulses were delivered at 20s intervals and 3 consecutive responses were averaged at each PPR test. The PPR was determined by the initial slope or amplitude of the second response over the first response in each pair. Since there was no significant difference between measurements in amplitude and initial slope, the data were pooled.

Frequency-dependent synaptic plasticity tests were performed at half-maximal fEPSP on each slice. After 20 min of slice acclimation, a ten-pulse stimulus train at 1.0, 5.0 or 10.0 Hz was applied to the Schaffer collaterals and the resultant responses were recorded. The slices were allowed to recover over 20 min before giving a different frequency stimulation. The 10 pulse-burst applied each time was at decreased inter-pulse intervals from 1.0 s to 0.2 s and then to 0.1 s, respectively. The initial slope from each pulse (2–10th pulses) in the recorded burst was analyzed and expressed as the percentage of the first pulse (taking the first pulse as 100%). The frequency facilitation (FF) of synaptic responses from the same experimental group at the same time point were analyzed and graphed.

2.5. Western blot analysis

Following treatment of reagents for 4 h, rat hippocampal slices were harvested for Western blot analysis. The lysates of brain tissue were prepared using RIPA lysis buffer (Thermo Fisher Scientific, Waltham, MA) supplemented with a protease inhibitor cocktail (Thermo Fisher Scientific). After quantification of protein concentrations with BCA protein assay kit (Thermo Fisher Scientific), 15 μg of total protein was loaded onto 8–12% SDS-

polyacrylamide gels, followed by the protocol as previously described (Liu et al., 2017; Xu et al., 2018). The primary antibodies used were BCL2-associated X protein (Bax; 1:500; Cell Signaling Technology), B cell lymphoma 2 (Bcl-2;1:1000; Cell Signaling Technology), caspase-1 (1:500; Santa Cruz), Iba-1 (1:500; FUJIFILM Wako), IL-1β (1:2500; Abcam), NLRP3 (1:500; Novusbio), ASC (1:500; Santa Cruz), caspase-8 (cas8; 1:500, Cell Signaling Technology), GAPDH (1:20000; Sigma), and β-actin (1:5000; Sigma). The immunoblots were detected by an enhanced chemiluminescence (ECL) system (Thermo Fisher Scientific) and imaged by the FluorChem M system (ProteinSimple, Santa Clara, CA). Band densities of labeled proteins were measured by ImageJ software (NIH, Bethesda, MD). The slices used for Western blotting study were not subjected to LTP experiments, but they were harvested in the same way as were for LTP experiments.

2.6. Immunofluorescence staining

After treatment with Meth and/or gp120 for 4 h, rat hippocampal slices were collected into 4% freshly made PFA (dissolved in 0.01 M PBS) overnight at 4 °C. Next day, the slices were moved into 10% sucrose for fixation until sinking to the bottom of EP tubes, followed by 20% and 30% sucrose in sequence in the same way. Then the optimum cutting temperature (O.C.T.) compound (Tissue-Tek® 4583, Sakura) was used to embed the slices on dry ice. Coronal sections of hippocampal embedded mass were cut at 10–20 μm in thickness using a freezing microtome (CM1850, Leica). After post-fixation in 4% PFA for 30 min, sections were washed with 0.01 M PBS three times, permeabilized in 0.01 M PBS containing 0.02% Triton X-100 (PBST) for 20 min, and then blocked in PBST containing 10% goat serum for 30 min at room temperature. Sections were then incubated in a humidified chamber overnight at 4 °C with the primary antibody (anti-CD11b: 1:200, AbD MCA275G; anti-Iba-1: 1:200, Wako 019–19,741; anti-ASC: 1:50, sc-514,414) in PBST with 10% goat serum. Next day, the sections were washed three times with PBST, followed by incubation 1 h with the secondary antibody (goat anti-mouse IgG H&L (Alexa Fluor® 488), 1:1000, ab150077; goat anti-mouse IgG H&L (Alexa Fluor® 594), 1:1000, A-11032; goat anti-rabbit IgG H&L (Alexa Fluor® 488), 1:1000, A-11034) in PBST solution at room temperature. Then 4′,6-diamidino-2-phenylindole (DAPI; 1:10000, Invitrogen™ D1306) in 0.01 M PBS was used to stain nuclei for 10 min. Finally, each slide was aspirated with the reagents and covered by a coverslip under the Fluoroshield Mounting Medium (P36934; Thermo Fisher Scientific). Images were acquired from the region of dentate gyrus by a confocal microscope (LSM 710; Zeiss). 10 regions of hippocampal slides in 4 rats were analyzed for each group, and quantified by ImageJ software (NIH, Bethesda, MD).

2.7. Statistical analyses

Statistical analyses were performed using GraphPad® Prism 9.0 (GraphPad Software, San Diego, CA). All data were graphed, and analyzed using one-way or two-way ANOVA, followed by Tukey's multiple comparisons test to determine significant group differences. Values were expressed as mean ± SEM and $p < 0.05$ was considered statistically significant. A portion of study on individual effect of Meth ($n = 8$) and gp120 ($n = 6$) on LTP were conducted in the presence of picrotoxin (20 μM) in the perfusate. Compared with the results of Meth ($n = 14$) and gp120 (n = 14) on LTP in the absence of picrotoxin in the perfusate,

there were no significant difference ($p > 0.05$). These data were combined for statistical analyses.

3. Results

3.1. Meth and gp120 inhibition of synaptic transmission in rat hippocampal slices

While the combined effects of Meth exposure and gp120 on synaptic function were examined in gp120 transgenic (gp120-tg) rodents, few studies have investigated their acute effects in the central nervous system (CNS). To explore their acute effects on synaptic transmission in the CNS, we examined I–O responses by electrical stimulation of Shafer-collateral fibers and recording of resultant fEPSPs in the CA1 dendritic field, using a protocol with a fixed IPI and variable stimulus current intensities from 0.2 mA to 0.8 mA in a 0.1 mA increment. Application of Meth (20 μM) and gp120 (200 pM) each alone onto the CA1 region of hippocampal slices significantly reduced average initial slopes at all stimulus intensities tested when compared with the average initial slope in control group ($F_{21, 605} = 7.948$, $P < 0.001$, Fig. 2). The average initial slope was further reduced when Meth and gp120 were administered in combination (Fig. 2). The reduction was statistically significant when compared with either Meth alone ($P_{0.7, 0.8} < 0.05$) or gp120 alone ($P_{0.6, 0.7} < 0.05$, $P_{0.8} < 0.01$) at different stimulus intensities, demonstrating synergistic effects of Meth and gp120 inhibition of synaptic transmission n

3.2. Meth augmentation of HIV-1 gp120 inhibition of LTP

Neurocognitive deficits tend to be worse in HIV-1-infected individuals with Meth abuse and the underlying mechanisms remain obscure. To explore the potential mechanisms for Meth exacerbation of neurocognitive deficits seen in HIV-1-infected individuals, we studied the effects of Meth (20 μM) and gp120 (200 pM) each alone and in combination on HFS-induced LTP in the CA3-CA1 synapses in rat hippocampal slices because memories are believed to be encoded by modification of synaptic strength and LTP is widely considered as one of the major cellular mechanisms underlying learning and memory. As shown in Figs. 3A–B, employment of the HFS protocol produced a robust LTP in untreated slices (control). The average magnitude of LTP was 237.68 ± 9.88% of baseline (Fig. 3C, Mean ± SEM, $n = 23$). Application of Meth and gp120 individually reduced LTP magnitudes to 156.35 ± 7.64% ($n = 22$) and 171.48 ± 6.89% ($n = 20$), respectively. The difference for each test was statistically significant compared to control ($P_{Meth} < 0.05$, $P_{gp120} < 0.001$). Application of Meth and gp120 in combination produced further significant reduction on LTP magnitude to 123.48 ± 4.09% ($p < 0.05$ vs Meth; $p < 0.001$ vs gp120, n = 20), demonstrating Meth potentiation of gp120-induced inhibition of LTP. Since Meth abuse could result in an increase of NLRP3 and induction of inflammation in the hippocampus of Meth users, we examined whether NLRP3 inflammasome activation was involved in the combined effects of Meth and gp120 on LTP. Local application of Ac-YVAD-CMK, a Caspase 1 inhibitor for 1 h significantly attenuated the combined effects of Meth and gp120 on LTP, indicating that activation of NLRP3 inflammasome was involved in the combined effects of Meth and gp120 on the inhibition of LTP. (Fig. 3C, $n = 10$). To mimic the stimulation under physiological condition, we employed widely used theta-burst stimulation (TBS) protocol and tested effects of Meth and gp120 on TBS-induced LTP. Likewise, TBS

also produced a robust LTP in the hippocampal slices (Fig. 3D). Meth and gp120 attenuated the average LTP magnitudes to 150.58 ± 28.14% (n = 6) and 156.09 ± 17.02% (n = 6) of baseline, respectively (Fig. 3E). In comparison to the LTP magnitude 273.94 ± 13.96% of baseline in control (n = 5), the differences were statistically significant ($p < 0.001$). Application of Meth and gp120 in combination further reduced LTP magnitude to 123.19 ± 8.46% of baseline (n = 7). Compared with the LTP magnitudes when Meth and gp120 were applied alone, the difference was statistically significant between Meth+gp120 and gp120 groups ($p < 0.05$), but not between Meth+gp120 and Meth groups ($p > 0.05$), demonstrating a synergic effect of Meth and gp120 on LTP in the hippocampal slices.

3.3. Meth- and gp120-alteration of paired-pulse ratio (PPR)

To understand the site of action of Meth and HIV-1 gp120 on synaptic transmission, we measured the PPR, the ratio of the fEPSP initial slope (or amplitude) of the second response over the first one. Paired-pulse stimulation with different IPIs produced robust responses in control slices as shown in Fig. 4A. Meth significantly increased PPR with stimulation IPIs of 40 ms (1.93 ± 0.05, n = 20 vs control: 1.63 ± 0.03, n = 20, $P < 0.01$; Figs. 4A–C), 60 ms (1.82 ± 0.05, n = 20 vs control: 1.57 ± 0.03, n = 20, $P < 0.05$; Fig. 4B) and 100 ms (1.67 ± 0.02, n = 20 vs control: 1.42 ± 0.02, n = 20, $P < 0.05$; Fig. 4B), while gp120 produced significant increase of PPR only in the IPI of 40 ms when compared to the control group (gp120: 1.89 ± 0.04, n = 20 vs control: 1.63 ± 0.03, n = 20, $P < 0.05$; Figs. 4A–C). These results suggested a presynaptic site of action for Meth and gp120. The PPR was further increased when Meth and gp120 were applied in combination, illustrating an augmented effect of Meth and gp120 on the PPR.

3.4. Effects of Meth and gp120 on frequency-dependent synaptic responses

In monosynaptic transmission, the magnitude of the postsynaptic responses evoked by pre-synaptic stimulation is intrinsically dependent on stimulation frequency (Markram et al., 1998). To examine whether Meth and gp120 alter frequency-dependent short-term synaptic plasticity in CA3-CA1 synapses, we recorded the fEPSPs elicited by a stimulation paradigm of ten-pulse train at the frequency of 1, 5 and 10 Hz, respectively (Fig. 5A). The responses evoked by the consecutive pulses in the train were quantified as the percent change of each of the nine consecutive fEPSPs with respect to the first fEPSP. Meth and gp120, applied alone or in combination, reduced the frequency-associated facilitation of synaptic response as reflected by the decrease of fEPSP slope at different frequencies (1 Hz: $F_{27, 666} = 1.53$, $P < 0.05$; 5 Hz: $F_{27, 666} = 1.31$, $P > 0.05$; 10 Hz: $F_{27, 657} = 6.49$, $P < 0.001$; Figs. 5B–D). At the tenth pulse of 10 Hz the reduction of frequency-associated facilitation of synaptic response was statistically significant compared to the control at 10 Hz ($P_{\text{Meth, Meth+gp120}} < 0.001$, $P_{\text{gp120}} < 0.05$, Fig. 5E), illustrating Meth and gp120 reduction of frequency-dependent synaptic response in the hippocampal brain slices. When applied in combination, Meth and gp120 were found to further reduce frequency facilitation of synaptic responses when compared to Meth alone at the frequency of 5 Hz (Meth+gp120: 145.15 ± 7.41%, n = 18 vs Meth: 175.1 ± 7.70%, n = 20, $p < 0.01$) or gp120 alone at 10 Hz (Meth+gp120: 151.48 ± 5.98%, n = 18 vs gp120: 184.53 ± 11.93%, n = 20, $p < 0.05$).

3.5. Activation of microglia in the hippocampus by Meth and gp120 in combination

Ample evidence indicates that microglia activation and resultant proinflammatory responses alter neuronal and synaptic function in the brain. To determine potential involvement of microglia activation in Meth- and gp120-associated inhibition of synaptic plasticity, we examined whether acute application of Meth and gp120 in the CA1 region produced microglia activation and resultant production of IL-1β in rat hippocampal slice. As shown in Figs. 6A–D, Meth and gp120 each alone induced microglia activation evidenced by an increase of CD11b/DAPI double positive cells in the hippocampus when compared to the control group ($P_{Meth} < 0.01$; $P_{gp120} < 0.05$). Most notably, remarkable increase in microglia activation was observed when Meth and gp120 were applied in combination ($P < 0.001$). The observed increase of microglia activation was in consistent with immunostaining, western blot results that the expression of Iba-1 protein, a microglia marker, and proIL-1β, a product of inflammatory response, were significantly upregulated by Meth and gp120 applied in combination (Figs. 6D–F). Application of LPS (100 ng/ml), a potent activator in inducing microglia activation, onto slices as a positive control also produced significant enhancement of the expression levels of Iba-1 and proIL-1β (Figs. 6D–F). To examine the potential involvement of inflammasome in Meth- and gp120-mediated microglial activation, a highly selective and irreversible caspase-1 inhibitor Ac-YVAD-CMK (10 μM) (Garcia-Calvo et al., 1998) was applied onto the hippocampus slices 1 h prior to the application of Meth+gp120. Under this experimental condition, microglial activation was markedly suppressed as evidenced by reduced expression levels of pro-IL-1β and Iba-1 (Figs. 6E–F, $P_{Iba\text{-}1} < 0.001$, $P_{IL\text{-}1\beta} < 0.01$), suggesting the involvement of inflammasome in Meth- and gp120-associated microglial activation.

3.6. Involvement of NLRP3 inflammasome in microglial activation induced by combined treatment of Meth and gp120

After observation on caspase-1 inhibitor Ac-YVAD-CMK suppression of microglia activation, we further analyzed the expression levels of inflammasome composition proteins by western blot and examined the adaptor protein ASC oligomerization in microglia using immunofluorescent staining. As a critical component of the inflammasome, ASC protein was found to aggregate, appearing as “speck”-like spots located at the nuclear periphery in microglia treated with Meth and gp120 (Fig. 7A). Such an aggregated ASC was only observed after treatment with Meth and gp120 in combination, but not in each treated alone, indicating the aggregation of inflammasome platform following treatment of Meth and gp120. To further examine the protein expression levels of inflammasome components, we also conduct western blot assay on hippocampal slices and exemplary gels were exhibited in Fig. 7B. As shown in Figs. 7D–E, upregulated levels of NLRP3, ASC and procaspase-1 were evident in Meth+gp120 group compared to the gp120-treated group ($p < 0.05$), and Meth-treated group ($p < 0.05$), respectively, indicating an involvement of NLRP3 inflammasome in microglia activatiion induced by Meth and gp120 applied in combination. LPS was tested as a positive control (Figs. 7B–E),

4. Discussion

Meth abuse and HIV-1 infection are two global public health issues. Being frequently comorbid with HIV-1 infection, Meth abuse exacerbates neurocognitive deficits in HIV-1-infected patients even in the era of cART (Chana et al., 2006; Chilunda et al., 2019; Kesby et al., 2015b). While many studies have investigated the individual effects of Meth and gp120 in the brain (Goldstein and Volkow, 2011; Thompson et al., 2004), far less has been focused on their synergistic influence. In the present study, we examined acute effects of Meth and gp120, when applied individually or in combination, on short- and long-term synaptic plasticity in the CA1 region of hippocampal slices prepared from young adult male Sprague-Dawley rats. Our results demonstrated that: (i) Meth and gp120 each alone attenuated short- and long-term synaptic plasticity as reflected by a decrease of I/O responses, a decline of fEPSP slope percentage in frequency tests, and a reduction on the magnitude of LTP induced by HFS and TBS in the presence of picrotoxin, a $GABA_A$ receptor antagonist; (ii) Meth augmented gp120-associated attenuation of short-and long-term synaptic plasticity when applied in combination; (iii) Meth and gp120 increased paired-pulse facilitation ratio, suggesting a presynaptic site of action; (iv) Meth and gp120 each alone or in combination induced significant microglia NLRP3 inflammasome activation in the hippocampus as revealed by increased expression levels of proIL-1β, NLRP3, ASC and procaspse-1; (v) application of Ac-YVAD-CMK, a potent and irreversible inhibitor of the inflammatory enzyme caspase-1 (Garcia-Calvo et al., 1998) blocked Meth+gp120-mediated attenuation of LTP, indicating an involvement of NLRP3 inflammasome activation in Meth- and gp120-associated attenuation of short- and long-term synaptic plasticity in the hippocampus.

The hippocampus has been a major brain system for studies of synaptic plasticity in the context of putative information-storage mechanisms in the brain. It is one of the most intensively investigated structure in the brain and activity-dependent synaptic plasticity is a prominent feature of hippocampal synapses. The most studied form of activity-dependent synaptic plasticity in the hippocampus is LTP, a widely accepted model linking synaptic plasticity with learning and memory (Neves et al., 2008; Takeuchi et al., 2014), although other forms of activity-dependent plasticity have also been found (Abraham et al., 1985; Dudek and Bear, 1992). Ample evidence indicates that the hippocampus is the primary site of spatial learning and long-term memory formation (Abraham et al., 2019; Brace et al., 1985). Alteration of hippocampal LTP induction may lead to impairment of learning and memory (Brace et al., 1985). To understand the mechanisms for Meth exacerbation of HAND seen in HIV-1-infected individuals with Meth abuse, we investigated acute effects of Meth and gp120 on synaptic transmission and plasticity in CA3 to CA1 synapses in the hippocampus, a brain region known to be vulnerable to HIV-1 infection (Kallianpur et al., 2013). Our results showed that localized application of Meth and gp120 each alone onto the CA1 region of the hippocampal slices reduced I–O responses and frequency facilitation, increased paired-pulse facilitation ratio, and attenuated LTP induced by HFS as well as by TBS. A synergistic augmentation on inhibition of synaptic transmission and plasticity was observed when Meth and gp120 were applied in combination. Alteration on paired-pulse facilitation ratio suggests presynaptic involvement in Meth- and gp120-mediated effects. The reduction of I–O responses and frequency facilitation is indicative of dysfunction of synaptic

transmission whereas the attenuation of LTP implies an impairment of learning and memory. The synergistic effects of Meth and gp120 revealed in this study may represent a potential mechanism, at least in part, for Meth-associated exacerbation of HAND observed clinically, even in the era of cART, in HIV-1-infected individuals with Meth dependence (Carey et al., 2006; Chana et al., 2006; Silverstein et al., 2012).

Much of the neurotoxicity associated with HIV-1 brain infection has been attributed to the effects of viral envelope protein gp120 shed off from infected cells. It has been demonstrated that gp120 causes neural cell apoptosis (Jana and Pahan, 2004) and oxidative stress (Price et al., 2005), disrupts blood-brain barrier (BBB) (Kanmogne et al., 2007) and induces neuroinflammation (Louboutin et al., 2010), ultimately leading to cognitive impairment and pathogenesis of HAND. In contrast to gp120, the neurotoxic effects of Meth, although well-studied, are not well-defined (Loftis and Janowsky, 2014; Shaerzadeh et al., 2018). While a plethora of research has investigated individual neurotoxic effects of gp120 and Meth in the brain, few have been done on their synergic influence on synaptic transmission and plasticity (LTP). In this study we observed that gp120, when applied alone, attenuated hippocampal LTP, which is consistent with the findings that gp120 inhibited short- and long-term potentiation in the hippocampus when applied acutely onto the hippocampal slices (Dong and Xiong, 2006; Shen et al., 2015), administered to the brain via intracerebroventricular infusion (for 3–5 days) (Sanchez-Alavez et al., 2000), or overexpressed in the brain in gp120-transgenic animals (Hoefer et al., 2015; Krucker et al., 1998). We also observed that Meth reduced LTP when applied acutely, which is in agreement with the results that Meth reduced LTP recorded either in the CA1 region of mouse hippocampus in vitro (Swant et al., 2010) and rat hippocampus ex vivo (Hori et al., 2010; Onaivi et al., 2002) or in the dentate gyrus in vivo in reinstated rats (Shahidi et al., 2019), along with the findings observed in the medial portion of the prefrontal cortex (Ishikawa et al., 2005) and in the cortical-striatal region of rats with self-administration of Meth (Huang et al., 2017). In addition to its suppressive effect, Meth was also found, when administered for a long-term with a low dose, to enhance LTP in differentiating and mature mouse dentate gyrus neural cells (Baptista et al., 2016). Nevertheless, limited studies have been done on their combined effects on LTP in the hippocampus. Current literature search on PubMed displayed only one publication investigated the combined effect of Meth and gp120 on LTP in HIV gp120-tg animals and that study demonstrated Meth enhanced gp120 reduction on LTP and impaired learning and memory (Hoefer et al., 2015). The results from that study can be utilized as a validation of acute effects of Meth and gp120 we observed in vitro in an animal model in vivo, solidifying Meth augmentation of gp120-associated attenuation of LTP in the hippocampus.

Mounting evidence indicates that Meth abuse exacerbates HAND in HIV-1-infected individuals (Carey et al., 2006; Chana et al., 2006). Animal models of neuroAIDS revealed that gp120 protein per se can cause cognitive impairment (Henry et al., 2013; Hoefer et al., 2015; Kesby et al., 2015b). Furthermore, a cross-species study demonstrated that HIV in humans and gp120 in mice impaired learning and executive functions which were worsened by Meth abuse in both species (Kesby et al., 2015b). Although exact mechanisms for Meth exacerbation of HIV/gp120-associated neurocognitive impairment remain ambiguous, various possibilities have been proposed including, but are not limited to, oxidative stress (Shah et al., 2013; Teodorof-Diedrich and Spector, 2020), microglia activation and resultant

neural injury (Chilunda et al., 2019; Liu et al., 2017; Xu et al., 2018), disruption of the blood-brain barrier (Mahajan et al., 2008; Ohene-Nyako et al., 2021) and synaptodendritic dysfunction and damage in the adult cortex and hippocampus (Hoefer et al., 2015; Thaney et al., 2018). Our results showed the synergic effect of Meth and gp120 on LTP was significantly attenuated by Ac-YVAD-CMK, a potent and irreversible inhibitor of the inflammatory enzyme caspase-1 (Garcia-Calvo et al., 1998). As the inflammasome consists of NLRP3 (receptor sensor), ASC (bridge protein) and Procaspase-1 (IL-1 converting enzyme), the Ac-YVAD-CMK-mediated attenuation of the synergic effect of Meth and gp120 on LTP suggests an involvement of NLRP3 inflammasome activation on Meth- and gp120- associated inhibition of LTP. Further studies revealed that Meth and gp120 induced microglia activation (Fig. 7) and increased the expression levels of Iba-1 and proIL-1β. The proIL-1β can be cleaved into IL-1β by caspase-1 and the elevated IL-1β may contribute to Meth and gp120-associated inhibition of LTP in the CA1 region of the hippocampus. This assumption is based on the fact that IL-1β receptors are present at high levels in the hippocampus (Parnet et al., 1994) and hippocampal LTP was impaired via mechanisms associated with microglial activation and IL-1β activity (Hoshino et al., 2017b; Hoshino et al., 2021). Indeed, many studies have demonstrated that IL-1β inhibits LTP in the hippocampus (Bellinger et al., 1993; Hoshino et al., 2017a; Katsuki et al., 1990; Schneider et al., 1998). In view of the results observed by others mentioned above and combined with our previous data that Meth induced inflammasome activation and increased production of IL-1β (Xu et al., 2018) and potentiated gp120-induced microglial activation in primary microglial cell cultures (Liu et al., 2017), we argue that Meth enhancement of gp120-associated microglial inflammasome activation may contribute to, at least in part, their inhibitory effects on synaptic transmission and plasticity in the hippocampus in vitro although further experiments are needed to test this argument.

It is worth pointing out that male rats were used in thw present study. Although estrous cycles might cause data variability the lack of including female animals in this study might cause unintentionally biased results because sex differences might exist in responding to Meth and gp120 challenges. Thus, the findings reported in this study might have a limitation in applying to both sexes. It is also worth pointing out that young adult animals were employed for the studies. The reason for choosing young adult animals was to minimize potential hypoxic/anoxic and surgical brain tissue damage because young animals are relatively more resistant to hypoxia/anoxia and easier for surgical dissecting brain out of cranial cavity. The results obtained from these young adult animals might have a limitation in implicating HIV-associated diseases in adulthood patients as well.

5. Conclusions

The present study demonstrated that Meth and gp120 each alone, when applied acutely, had an inhibitory effect on short-term and long-term synaptic plasticity in the CA1 region of rat hippocampal slices as revealed by tests on IO responses, frequency facilitation and LTP. Meth augmented gp120 inhibition of synaptic plasticity when applied in combination. Changes in paired-pulse facilitation suggest presynaptic involvement in Meth- and gp120-associated actions. The synergic effects of Meth and gp120 on LTP was blocked by Ac-YVAD-CMK, a potent inhibitor of the inflammatory enzyme caspase-1, suggesting an

involvement of NLRP3 inflammasome activation in Meth augmentation of gp120 reduction of LTP in the hippocampus. The results obtained in the present study may implicate a potential mechanism, at least in part, for Meth-associated exacerbation of HAND observed in HIV-1-infected individuals with Meth dependence in the era of cART.

Acknowledgements

Our thanks to Mr. Reed Felderman for critical reading of the manuscript, and to Ms. Kimberly S. Morrison and Ms. Karalyn A. Schmidt for their administrative supports during the research. The authors also thank two anonymous reviewers for their constructive criticisms, comments, and suggestions.

Funding and disclosures

This work was supported by the grant R01DA050540 (H.X.) from National Institute on Drug Abuse, National Institutes of Health. Y. Z. was supported by a Scholarship from China Scholarship Council (CSC) Joint-Training Scholarship Program.

Data and materials availability

The data that support the findings of this study are available from corresponding author upon reasonable request.

References

Abraham WC, et al. , 1985. Heterosynaptic changes accompany long-term but not short-term potentiation of the perforant path in the anaesthetized rat. J. Physiol 363, 335–349. [PubMed: 2991506]

Abraham WC, et al. , 2019. Is plasticity of synapses the mechanism of long-term memory storage? NPJ Sci Learn 4, 9. [PubMed: 31285847]

Antinori A, et al. , 2007. Updated research nosology for HIV-associated neurocognitive disorders. Neurology 69, 1789–1799. [PubMed: 17914061]

Baptista S, et al. , 2016. Long-term treatment with low doses of methamphetamine promotes neuronal differentiation and strengthens long-term potentiation of glutamatergic synapses onto dentate granule neurons. eNeuro 3.

Bellinger FP, et al. , 1993. Interleukin 1 beta inhibits synaptic strength and long-term potentiation in the rat CA1 hippocampus. Brain Res 628, 227–234. [PubMed: 8313151]

Bird CM, Burgess N, 2008. The hippocampus and memory: insights from spatial processing. Nat. Rev. Neurosci 9, 182–194. [PubMed: 18270514]

Brace HM, et al. , 1985. Long-term changes in hippocampal physiology and learning ability of rats after intrahippocampal tetanus toxin. J. Physiol 368, 343–357. [PubMed: 4078743]

Carey CL, et al. , 2006. Additive deleterious effects of methamphetamine dependence and immunosuppression on neuropsychological functioning in HIV infection. AIDS Behav 10, 185–190. [PubMed: 16477511]

Castelo JM, et al. , 2006. Altered hippocampal-prefrontal activation in HIV patients during episodic memory encoding. Neurology 66, 1688–1695. [PubMed: 16769942]

Chana G, et al. , 2006. Cognitive deficits and degeneration of interneurons in HIV+ methamphetamine users. Neurology 67, 1486–1489. [PubMed: 17060582]

Chilunda V, et al. , 2019. The impact of substance abuse on HIV-mediated neuropathogenesis in the current ART era. Brain Res 1724, 146426. [PubMed: 31473221]

Cummins NW, et al. , 2010. How much gp120 is there? J. Infect. Dis 201, 1273–1274 (author reply 1274–5). [PubMed: 20225961]

Dong J, Xiong H, 2006. Human immunodeficiency virus type 1 gp120 inhibits long-term potentiation via chemokine receptor CXCR4 in rat hippocampal slices. J. Neurosci. Res 83, 489–496. [PubMed: 16400660]

Du L, et al. , 2019. Involvement of NLRP3 inflammasome in methamphetamine-induced microglial activation through miR-143/PUMA axis. Toxicol. Lett 301, 53–63. [PubMed: 30394308]

Dudek SM, Bear MF, 1992. Homosynaptic long-term depression in area CA1 of hippocampus and effects of N-methyl-D-aspartate receptor blockade. Proc. Natl. Acad. Sci. U. S. A 89, 4363–4367. [PubMed: 1350090]

Garcia-Calvo M, et al. , 1998. Inhibition of human caspases by peptide-based and macromolecular inhibitors. J. Biol. Chem 273, 32608–32613. [PubMed: 9829999]

Gilbert PB, et al. , 2003. Long-term safety analysis of preventive HIV-1 vaccines evaluated in AIDS vaccine evaluation group NIAID-sponsored phase I and II clinical trials. Vaccine 21, 2933–2947. [PubMed: 12798637]

Goldstein RZ, Volkow ND, 2011. Dysfunction of the prefrontal cortex in addiction: neuroimaging findings and clinical implications. Nat. Rev. Neurosci 12, 652–669. [PubMed: 22011681]

Gonzales R, et al. , 2010. The methamphetamine problem in the United States. Annu. Rev. Public Health 31, 385–398. [PubMed: 20070191]

He X, et al. , 2020. NLRP3-dependent pyroptosis is required for HIV-1 gp120-induced neuropathology. Cell. Mol. Immunol 17, 283–299. [PubMed: 31320730]

Heaton RK, et al. , 2011. HIV-associated neurocognitive disorders before and during the era of combination antiretroviral therapy: differences in rates, nature, and predictors. J. Neuro-Oncol 17, 3–16.

Henry BL, et al. , 2013. Behavioral effects of chronic methamphetamine treatment in HIV-1 gp120 transgenic mice. Behav. Brain Res 236, 210–220. [PubMed: 22960458]

Hoefer MM, et al. , 2015. Combination of methamphetamine and HIV-1 gp120 causes distinct long-term alterations of behavior, gene expression, and injury in the central nervous system. Exp. Neurol 263, 221–234. [PubMed: 25246228]

Hori N, et al. , 2010. Neurotoxic effects of methamphetamine on rat hippocampus pyramidal neurons. Cell. Mol. Neurobiol 30, 849–856. [PubMed: 20232135]

Hoshino K, et al. , 2017a. Synapse-specific effects of IL-1beta on long-term potentiation in the mouse hippocampus. Biomed. Res 38, 183–188. [PubMed: 28637953]

Hoshino K, et al. , 2017b. Minocycline prevents the impairment of hippocampal long-term potentiation in the septic mouse. Shock 48, 209–214. [PubMed: 28187038]

Hoshino K, et al. , 2021. Interleukin-1beta modulates synaptic transmission and synaptic plasticity during the acute phase of Sepsis in the senescence-accelerated mouse Hippocampus. Front. Aging Neurosci 13, 637703. [PubMed: 33643027]

Huang X, et al. , 2017. Methamphetamine abuse impairs motor cortical plasticity and function. Mol. Psychiatry 22, 1274–1281. [PubMed: 28831198]

Ishikawa A, et al. , 2005. Essential role of D1 but not D2 receptors in methamphetamine-induced impairment of long-term potentiation in hippocampal-prefrontal cortex pathway. Eur. J. Neurosci 22, 1713–1719. [PubMed: 16197511]

Jana A, Pahan K, 2004. Human immunodeficiency virus type 1 gp120 induces apoptosis in human primary neurons through redox-regulated activation of neutral sphingomyelinase. J. Neurosci 24, 9531–9540. [PubMed: 15509740]

Kallianpur KJ, et al. , 2013. Peripheral blood HIV DNA is associated with atrophy of cerebellar and subcortical gray matter. Neurology 80, 1792–1799. [PubMed: 23596064]

Kanmogne GD, et al. , 2007. HIV-1 gp120 compromises blood-brain barrier integrity and enhances monocyte migration across blood-brain barrier: implication for viral neuropathogenesis. J. Cereb. Blood Flow Metab 27, 123–134. [PubMed: 16685256]

Kapadia F, et al. , 2005. The role of substance abuse in HIV disease progression: reconciling differences from laboratory and epidemiologic investigations. Clin. Infect. Dis 41, 1027–1034. [PubMed: 16142670]

Katsuki H, et al. , 1990. Interleukin-1 beta inhibits long-term potentiation in the CA3 region of mouse hippocampal slices. Eur. J. Pharmacol 181, 323–326. [PubMed: 2166677]

Kelschenbach J, et al. , 2019. Efficient expression of HIV in immunocompetent mouse brain reveals a novel nonneurotoxic viral function in hippocampal synaptodendritic injury and memory impairment. mBio 10.

Kesby JP, et al. , 2015a. Methamphetamine exposure combined with HIV-1 disease or gp120 expression: comparison of learning and executive functions in humans and mice. Neuropsychopharmacology 40, 1899–1909. [PubMed: 25652249]

Kesby JP, et al. , 2015b. Cognitive deficits associated with combined HIV gp120 expression and chronic methamphetamine exposure in mice. Eur. Neuropsychopharmacol. J. Eur. College Neuropsychopharmacol 25, 141–150.

Klasse PJ, Moore JP, 2004. Is there enough gp120 in the body fluids of HIV-1-infected individuals to have biologically significant effects? Virology 323, 1–8. [PubMed: 15165814]

Knierim JJ, 2015. The hippocampus. Curr. Biol 25, R1116–R1121. [PubMed: 26654366]

Krucker T, et al. , 1998. Transgenic mice with cerebral expression of human immunodeficiency virus type-1 coat protein gp120 show divergent changes in short-and long-term potentiation in CA1 hippocampus. Neuroscience 83, 691–700. [PubMed: 9483553]

Lanman T, et al. , 2021. CNS neurotoxicity of antiretrovirals. J. NeuroImmune Pharmacol 16, 130–143. [PubMed: 31823251]

Larsen KE, et al. , 2002. Methamphetamine-induced degeneration of dopaminergic neurons involves autophagy and upregulation of dopamine synthesis. J. Neurosci 22, 8951–8960. [PubMed: 12388602]

Liu J, et al. , 2017. Methamphetamine potentiates HIV-1gp120-induced microglial neurotoxic activity by enhancing microglial outward K(+) current. Mol. Cell. Neurosci 82, 167–175. [PubMed: 28552341]

Loftis JM, Janowsky A, 2014. Neuroimmune basis of methamphetamine toxicity. Int. Rev. Neurobiol 118, 165–197. [PubMed: 25175865]

Louboutin JP, et al. , 2010. HIV-1 gp120-induced neuroinflammation: relationship to neuron loss and protection by rSV40-delivered antioxidant enzymes. Exp. Neurol 221, 231–245. [PubMed: 19913017]

Mahajan SD, et al. , 2008. Methamphetamine alters blood brain barrier permeability via the modulation of tight junction expression: implication for HIV-1 neuropathogenesis in the context of drug abuse. Brain Res 1203, 133–148. [PubMed: 18329007]

Mahmoudiasl GR, et al. , 2019. Nod-like receptor protein 3 and nod-like receptor protein 1 inflammasome activation in the hippocampal region of postmortem methamphetamine chronic user. Bratisl. Lek. Listy 120, 769–776. [PubMed: 31663353]

Markram H, et al. , 1998. Information processing with frequency-dependent synaptic connections. Neurobiol. Learn. Mem 70, 101–112. [PubMed: 9753590]

Marquez C, et al. , 2009. Methamphetamine use, sexual activity, patient-provider communication, and medication adherence among HIV-infected patients in care, San Francisco 2004–2006. AIDS Care 21, 575–582. [PubMed: 19444665]

Mattson MP, et al. , 2005. Cell death in HIV dementia. Cell Death Differ 12 (Suppl. 1), 893–904. [PubMed: 15761472]

McIntosh RC, et al. , 2015. Neuropathological sequelae of human immunodeficiency virus and apathy: a review of neuropsychological and neuroimaging studies. Neurosci. Biobehav. Rev 55, 147–164. [PubMed: 25944459]

Mitchell SJ, et al. , 2006. Methamphetamine use and sexual activity among HIV-infected patients in care–San Francisco, 2004. AIDS Patient Care STDs 20, 502–510. [PubMed: 16839249]

Morgan SL, Teyler TJ, 2001. Electrical stimuli patterned after the theta-rhythm induce multiple forms of LTP. J. Neurophysiol 86, 1289–1296. [PubMed: 11535677]

Navia BA, et al. , 1986. The AIDS dementia complex: II. Neuropathology. Ann. Neurol 19, 525–535. [PubMed: 3014994]

Neves G, et al. , 2008. Synaptic plasticity, memory and the hippocampus: a neural network approach to causality. Nat. Rev. Neurosci 9, 65–75. [PubMed: 18094707]

Oh SK, et al. , 1992. Identification of HIV-1 envelope glycoprotein in the serum of AIDS and ARC patients. J. Acquir. Immune Defic. Syndr 5, 251–256. [PubMed: 1740750]

Ohene-Nyako M, et al. , 2021. Hippocampal blood-brain barrier of methamphetamine self-administering HIV-1 transgenic rats. Eur. J. Neurosci 53, 416–429. [PubMed: 32725911]

Onaivi ES, et al. , 2002. Ibogaine signals addiction genes and methamphetamine alteration of long-term potentiation. Ann. N. Y. Acad. Sci 965, 28–46. [PubMed: 12105083]

Parnet P, et al. , 1994. Expression of type I and type II interleukin-1 receptors in mouse brain. Brain Res. Mol. Brain Res 27, 63–70. [PubMed: 7877456]

Price TO, et al. , 2005. HIV-1 viral proteins gp120 and tat induce oxidative stress in brain endothelial cells. Brain Res 1045, 57–63. [PubMed: 15910762]

Sanchez AB, Kaul M, 2017. Neuronal stress and injury caused by HIV-1, cART and drug abuse: converging contributions to HAND. Brain Sci 7.

Sanchez AB, et al. , 2015. Antiretrovirals, methamphetamine, and HIV-1 envelope protein gp120 compromise neuronal energy homeostasis in association with various degrees of synaptic and neuritic damage. Antimicrob. Agents Chemother 60, 168–179. [PubMed: 26482305]

Sanchez-Alavez M, et al. , 2000. HIV- and FIV-derived gp120 alter spatial memory, LTP, and sleep in rats. Neurobiol. Dis 7, 384–394. [PubMed: 10964609]

Santosuosso M, et al. , 2009. HIV-1 envelope protein gp120 is present at high concentrations in secondary lymphoid organs of individuals with chronic HIV-1 infection. J. Infect. Dis 200, 1050–1053. [PubMed: 19698075]

Saylor D, et al. , 2016. HIV-associated neurocognitive disorder - pathogenesis and prospects for treatment. Nat. Rev. Neurol 12, 309. [PubMed: 27080521]

Schneider H, et al. , 1998. A neuromodulatory role of interleukin-1beta in the hippocampus. Proc. Natl. Acad. Sci. U. S. A 95, 7778–7783. [PubMed: 9636227]

Shaerzadeh F, et al. , 2018. Methamphetamine neurotoxicity, microglia, and neuroinflammation. J. Neuroinflammation 15, 341. [PubMed: 30541633]

Shah A, et al. , 2013. HIV gp120- and methamphetamine-mediated oxidative stress induces astrocyte apoptosis via cytochrome P450 2E1. Cell Death Dis 4, e850. [PubMed: 24113184]

Shahidi S, et al. , 2019. Different doses of methamphetamine alter long-term potentiation, level of BDNF and neuronal apoptosis in the hippocampus of reinstated rats. J. Physiol. Sci 69, 409–419. [PubMed: 30680641]

Shen LL, et al. , 2015. Curcumin improves synaptic plasticity impairment induced by HIV-1gp120 V3 loop. Neural Regen. Res 10, 925–931. [PubMed: 26199609]

Silverstein PS, et al. , 2012. HIV-1 gp120 and drugs of abuse: interactions in the central nervous system. Curr. HIV Res 10, 369–383. [PubMed: 22591361]

Smith LK, et al. , 2018. HIV associated neurodegenerative disorders: a new perspective on the role of lipid rafts in Gp120-mediated neurotoxicity. Curr. HIV Res 16, 258–269. [PubMed: 30280668]

Swant J, et al. , 2010. Methamphetamine reduces LTP and increases baseline synaptic transmission in the CA1 region of mouse hippocampus. PLoS One 5, e11382. [PubMed: 20614033]

Takeuchi T, et al. , 2014. The synaptic plasticity and memory hypothesis: encoding, storage and persistence. Philos. Trans. R. Soc. Lond. Ser. B Biol. Sci 369, 20130288. [PubMed: 24298167]

Teodorof-Diedrich C, Spector SA, 2020. Human immunodeficiency virus type 1 and methamphetamine-mediated mitochondrial damage and neuronal degeneration in human neurons. J. Virol 94.

Thaney VE, et al. , 2018. Transgenic mice expressing HIV-1 envelope protein gp120 in the brain as an animal model in neuroAIDS research. J. Neuro-Oncol 24, 156–167.

Thompson PM, et al. , 2004. Structural abnormalities in the brains of human subjects who use methamphetamine. J. Neurosci 24, 6028–6036. [PubMed: 15229250]

Timilsina U, Gaur R, 2016. Modulation of apoptosis and viral latency - an axis to be well understood for successful cure of human immunodeficiency virus. J Gen Virol 97, 813–824. [PubMed: 26764023]

Trujillo JR, et al. , 1996. High levels of anti-HIV-1 envelope antibodies in cerebrospinal fluid as compared to serum from patients with AIDS dementia complex. J Acquir Immune Defic Syndr Hum Retrovirol 12, 19–25. [PubMed: 8624756]

Walsh JG, et al. , 2014. Rapid inflammasome activation in microglia contributes to brain disease in HIV/AIDS. Retrovirology 11, 35. [PubMed: 24886384]

Xiong H, et al. , 1996. Brain-derived peptides inhibit synaptic transmission via presynaptic GABAB receptors in CA1 area of rat hippocampal slices. Brain Res 737, 188–194. [PubMed: 8930365]

Xu E, et al. , 2018. Inflammasome activation by methamphetamine potentiates lipopolysaccharide stimulation of IL-1beta production in microglia. J. NeuroImmune Pharmacol 13, 237–253. [PubMed: 29492824]

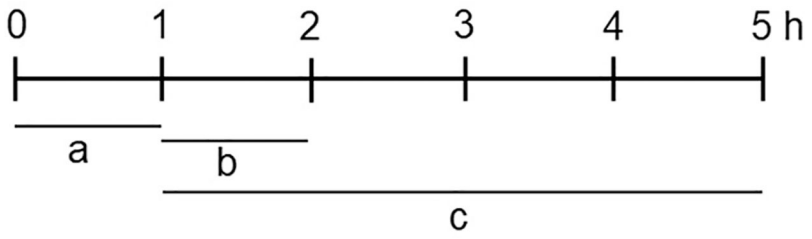

Fig. 1.

Experimental timeline. a. After harvesting the slices were allowed to recover for 1 h in an interface incubation chamber before being selected for experimental treatments. b. Slices were treated for 1 h, unless otherwise stated, with Meth and gp120 each alone, or Meth+gp120, Meth+gp120+ Ac-YVAD-CMK before being used electrophysiology experiments. c. Slices were treated for 4 h with Meth, gp120 and LPS each alone, or Meth+gp120, Meth+gp120+ Ac-YVAD-CMK before being collected for IHC and/or Western blot experiments.

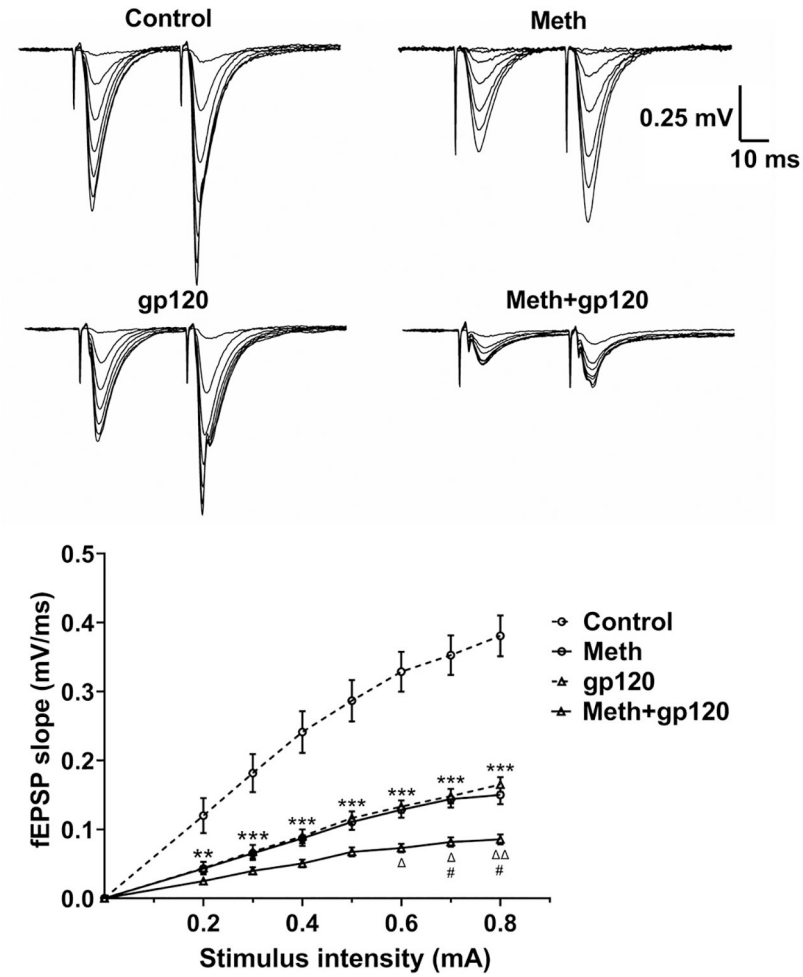

Fig. 2.

Inhibitory effects of Meth and HIV-1 gp120 on synaptic transmission in the CA1 region of rat hippocampal slices.

Upper panel: Representative input-output traces of superimposed fEPSPs, evoked by twin-pulse stimuli (10 μs in duration, 40 ms inter-pulse interval) at various intensities ranging from 0.2 to 0.8 mA with an increment of 0.1 mA, were recorded from hippocampal slices with different treatments as indicated. Each trace shown was an average of consecutive 3 evoked fEPSPs. Lower panel: Averaged input-output curves generated by plotting fEPSP initial slope of the first pulse against the stimulus intensities ranging from 0.2 to 0.8 mA as shown in A. Note that Meth and gp120 each alone significantly decreased the slopes of fEPSP evoked by stimuli with all different intensities. Combined application further deceased the fEPSP slope at stimulus intensity of 0.7 mA compared to Meth alone, and at 0.6 mA, 0.7 mA and 0.8 mA compared to gp120 alone. Data represent mean ± SEM with n = 20 in each group and are analyzed using two-way ANOVA followed by Tukey's post hoc test. $^{**}P < 0.01$, $^{***}P < 0.001$ vs. control, $^{\#}P < 0.05$ vs. Meth. $^{\Delta}P < 0.05$, $^{\Delta\Delta}P < 0.001$ vs. gp120.

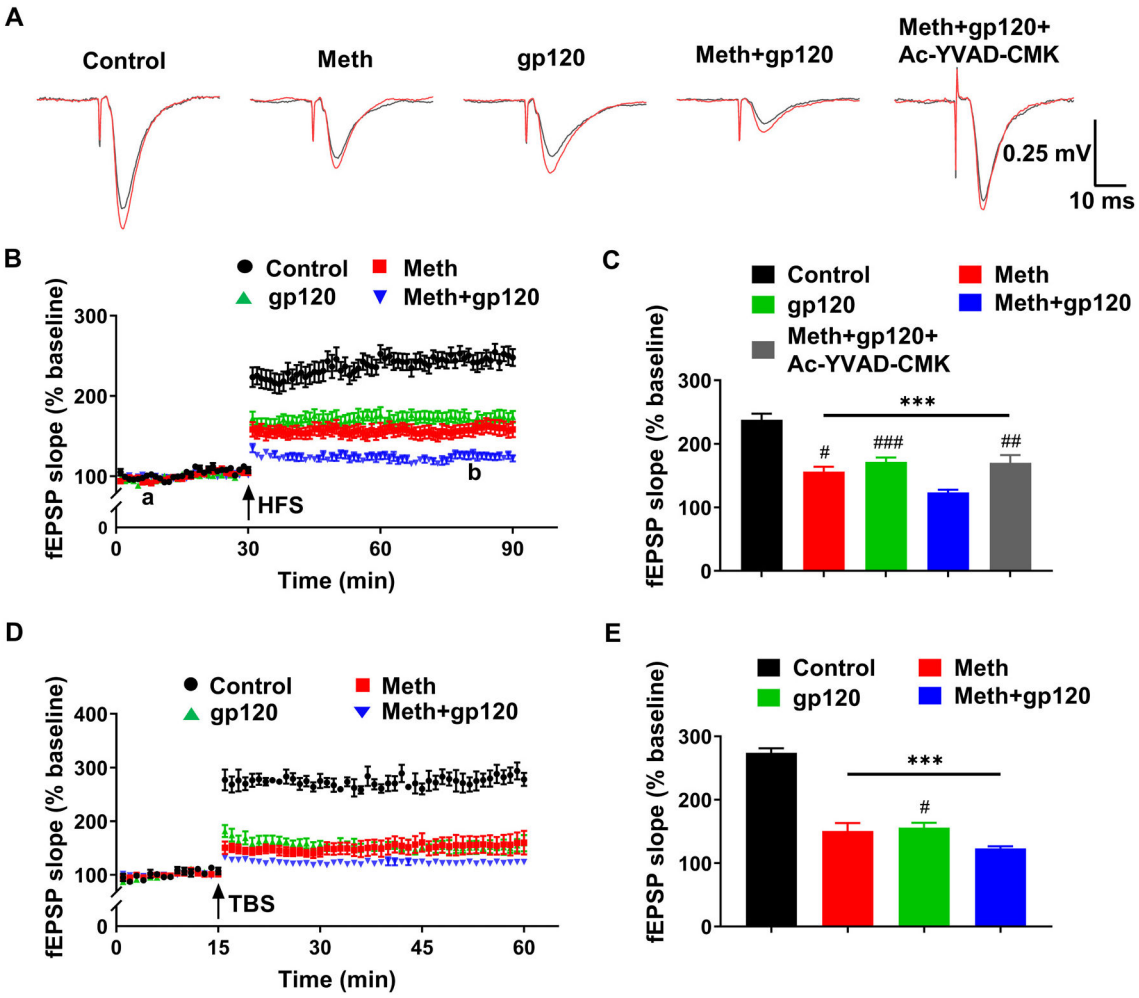

Fig. 3.

Meth augments HIV-1 gp120 inhibition of long-term potentiation (LTP) induced by either high-frequency stimulation (HFS) or theta-burst stimulation (TBS). Panel A shows the representative fEPSPs taken at the time points of *a* (base line, in black) and *b* (50 min after HFS, in red) at different experimental condition as shown in Panel B. Panels B and D illustrate the time courses and average magnitudes of LTP recorded in the Schaffer-collateral to CA1 synapses induced by HFS (B) or TBS (D) under different experimental conditions as indicated. Note that the time course and average magnitudes of LTP for Meth+gp120 + Ac-YVAD-CMK group were not shown in Panel B due to over-crowed curves and overlap. Panels C and E are summarized bar graphs for Panels B and D respectively, showing that Meth and gp120 each alone significantly reduced the magnitude (an average of 60 min LTP) of LTP induced by HFS (C) and TBS (E). However, Meth augmented gp120 reduction of LTP magnitude when tested in combination. Addition of caspase 1 inhibitor Ac-YVAD-CMK blocked Meth-associated augmentation of gp120 reduction on LTP magnitude, suggesting an involvement of inflammasome in such an augmentation. Sample size (n) in groups of HFS and TBS (in brackets): Control 23 (5), Meth 22 (6), gp120 20 (6), Meth+gp120 20 (7), Meth+gp120 + Ac-YVAD-CMK 10. Data represent the mean

± SEM and are analyzed using one-way or two-way ANOVA followed by Tukey's multiple comparisons test. ***$P < 0.001$ vs. control, $^{\#\#}P < 0.01$, $^{\#\#\#}P < 0.001$ vs. Meth+gp120.

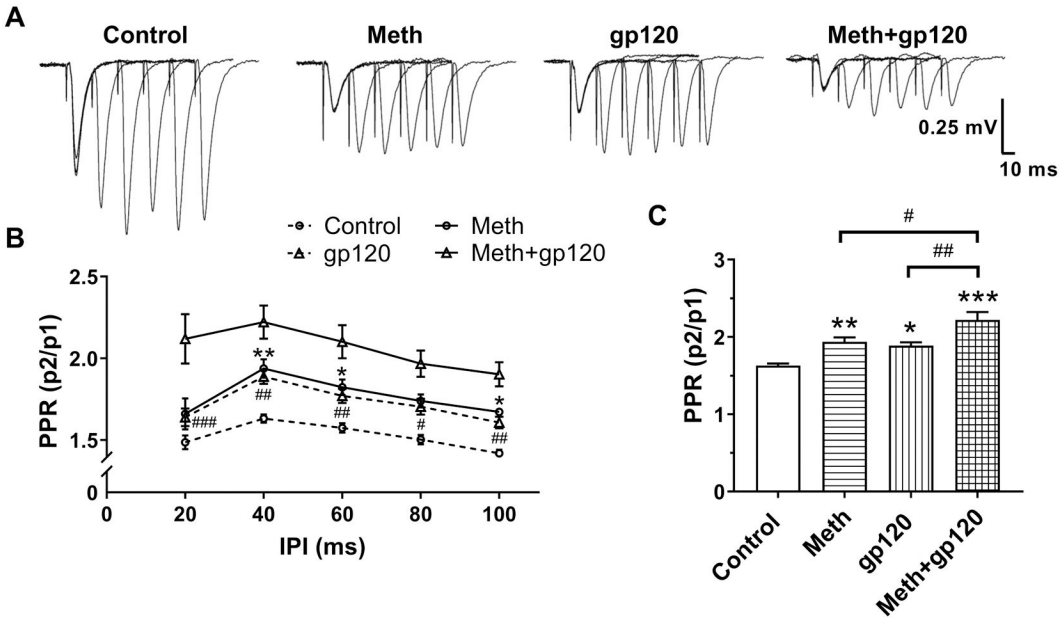

Fig. 4.

Meth- and gp120-induced alteration of PPR.

Effects of Meth and gp120 on PPR were tested at the Schaffer-collateral to CA1 synapses in the hippocampal slices. fEPSPs were elicited by paired-pulse stimulation (10 μs in duration, 200 μA in intensity) with varying inter-pulse interval (IPI) from 20 to 100 ms with an increment of 20 ms. The PPRwas calculated by dividing the initial slope (or peak amplitude) of the first fEPSP from that of the second fEPSP. (A) Representative superimposed traces of fEPSPs recorded at indicated experimental conditions in response to paired-pulse stimulations with different IPIs. (B) Line graph plots the magnitudes of PPRs against IPIs. Note a decrease in second responses as IPI increase starting from 40 ms. (C) Bar graph shows the PPRs at 40 ms IPI in different experimental conditions. Note Meth and g120 each alone increased PPR and a further significant increase in PPR was observed when Meth and gp120 was tested in combination, illustrating a presynaptic site of action. Data represent the mean ± SEM with n = 20 in each group and were analyzed using two-way ANOVA (B) and one-way ANOVA followed by Tukey's post hoc test (C). $^{*}P < 0.05$, $^{**}P < 0.01$, $^{***}P < 0.001$ vs. control, $^{\#}P < 0.05$, $^{\#\#}P < 0.01$, $^{\#\#\#}P < 0.001$ vs. Meth+gp120.

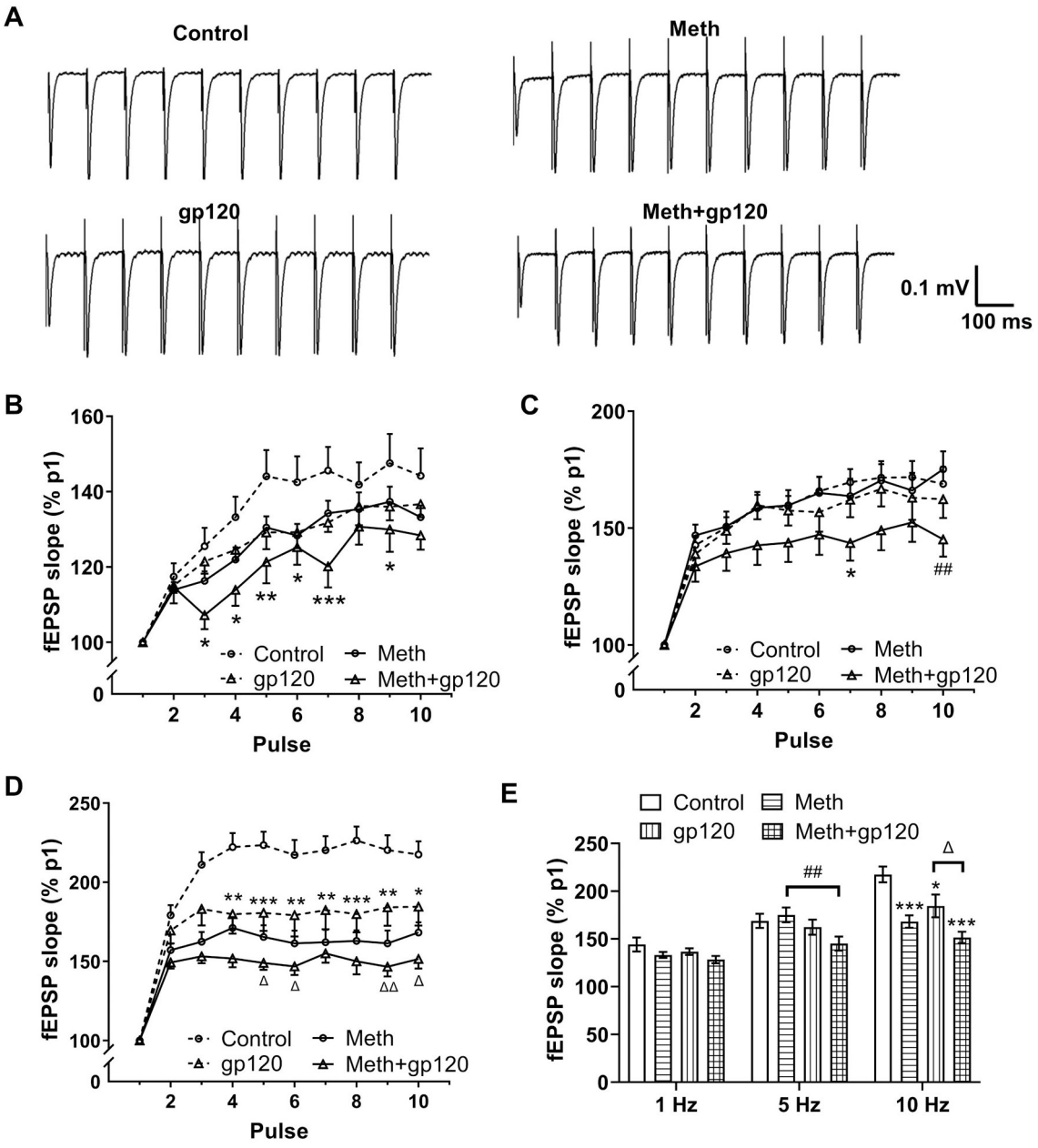

Fig. 5.

Meth- and gp120-associated alteration of frequency facilitation (FF) of synaptic responses. The influence of Meth and gp120 on FF of synaptic responses were examined in the CA1 region of hippocampal slices. Comparisons were made among frequency responses generated in response to a 10-pulse stimulation (10 μs in duration, 0.2 mA in intensity,) at 1.0 Hz, 5.0 Hz and 10.0 Hz. The degree of facilitation was expressed as the percentage of initial slopes of the 2–10th pulses over the first one (regarding the first pulse as 100%). (A) Exemplary FF recordings at the frequency of 10 Hz from four experimental conditions. Each trace shown was an average of consecutive 3 evoked fEPSPs. (B), (C) and (D) are line graphs exhibiting average normalized fEPSP slopes at the corresponding frequency of 1 Hz, 5 Hz, and 10 Hz. Note significant reductions of FF in some pulses in Meth+gp120 group

(n = 18) compared to control (n = 20). (E) Summary data of tenth fEPSP slopes obtained at four distinct experimental conditions with different stimulation frequencies. Note that at 10 Hz, Meth (n = 20) and gp120 (n = 20), applied alone or in combination, decreased FF dramatically when compared with gp120 alone, demonstrating Meth and gp120 impairment of FF in the hippocampus. Data represent the mean ± SEM and are analyzed using two-way ANOVA followed by Tukey's post hoc test. $^{*}P < 0.05$, $^{**}P < 0.01$, $^{***}P < 0.001$ vs. control, $^{\#\#}P < 0.01$ vs. Meth, $^{\Delta}P < 0.05$, $^{\Delta\Delta}P < 0.01$ vs. gp120.

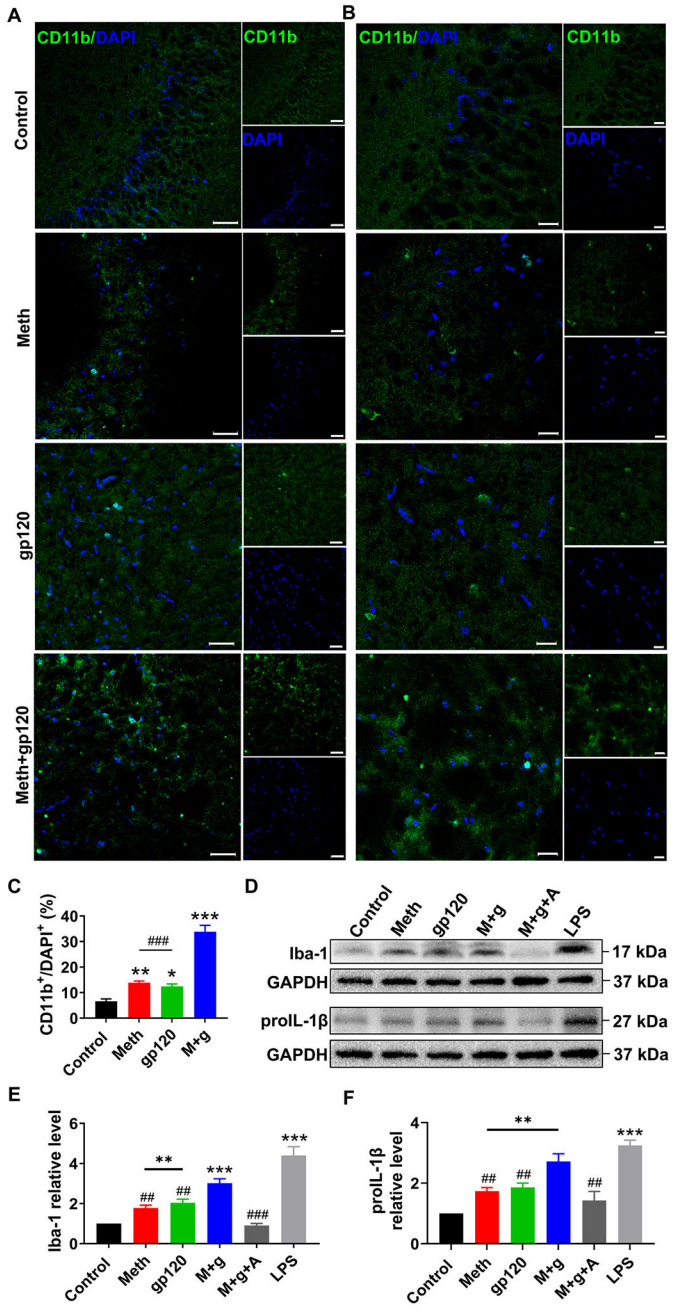

Fig. 6.

Meth- and gp120-induced microglial activation in hippocampal slices.

(A) Immunostaining displays expression of CD11b, a marker of microglial activation, in the rat hippocampal slices in experimental groups as indicated. The right two images (vertical) in each group were the images of CD11b staining (green, upper) and DAPI staining (blue, lower). The left image (larger in size) in each group was an enlarged photo with CD11b-staining image and DAPI-staining image superimposed. Images were visualized by fluorescent microscopy at x20 original magnification. Scale bar equals 50 μm. (B) Representative images, from each group shown in (A), *were* visualized by fluorescent

microscopy at x40 original magnification. Scale bar equals 20 μm. (C) Bar graph exhibiting quantification of $CD11b^+/DAPI^+$ cells showed that microglial activation was significantly potentiated by Meth and gp120 applied in combination (M+g). $N = 10$ in each group (4 independent experiments). (D) Exemplary bands of western blot analysis illustrated the expression levels of Iba-1 and proIL-1β. (*E*-F) Bar graphs showing band densitometry data in ($n = 8$ in each group, 4 independent experiments). Application of Meth and gp120 each alone significantly ($p < 0.01$) increased the expression levels of Iba-1 and proIL-1β. However, a more significant increase ($p < 0.001$) was observed when applied in combination (M+g). Note that pretreatment of slices with caspase-1 inhibitor Ac-YVAD-CMK (10 μM) for 1 h blocked the combined effect of Meth and gp120 (M+g+A). Lipopolysaccharide (LPS, 100 ng/ml) was tested as a positive control. Data are presented as mean ± SEM and analyzed by one-way ANOVA followed by Turkey's post hoc test. * $p < 0.05$, ** $p < 0.01$, *** $p < 0.001$ vs. control, $^{\#\#}p < 0.01$, $^{\#\#\#}P < 0.001$ vs. Meth+gp120.

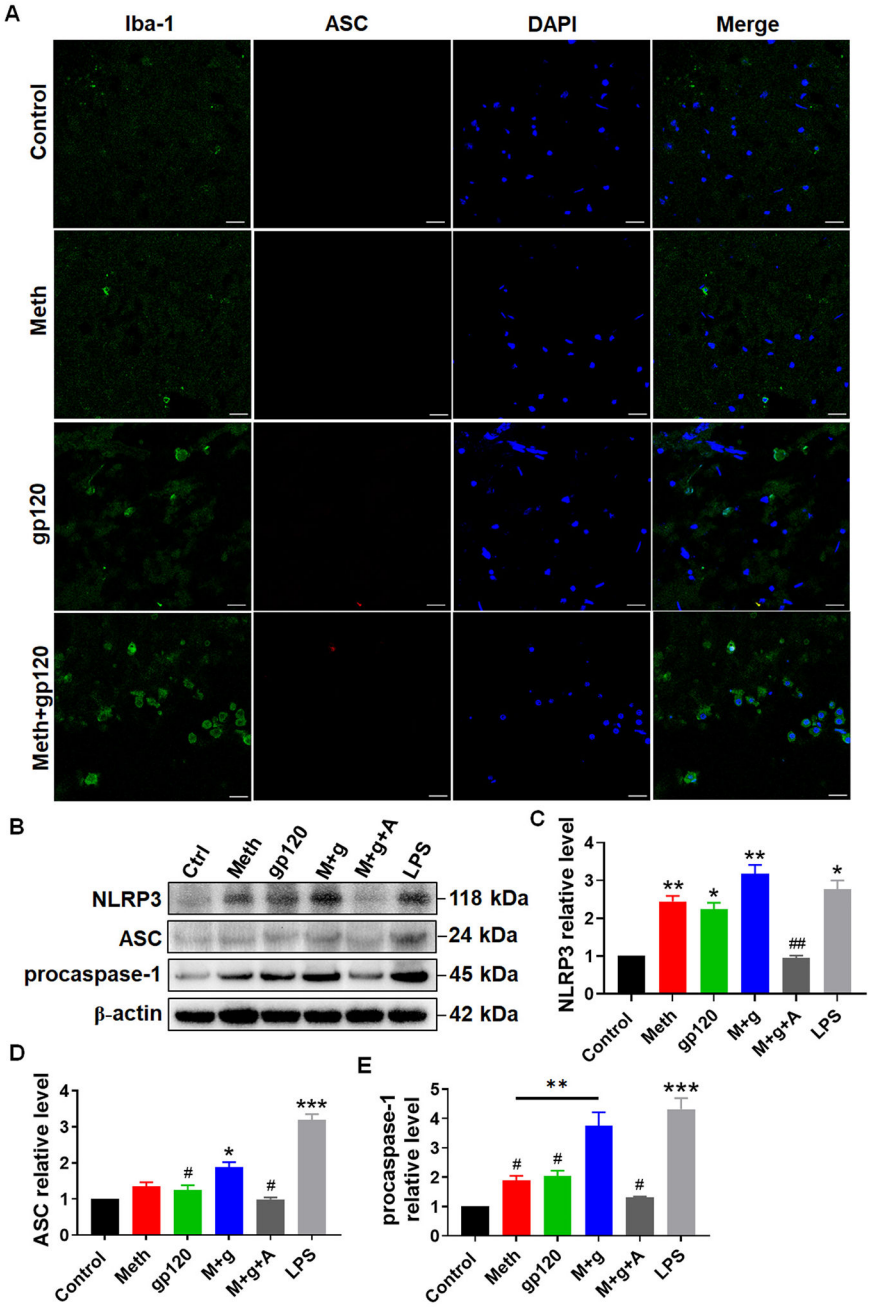

Fig. 7.

Involvement of NLRP3 inflammasome in synergic microglial activation by Meth and gp120. (A) Representative immunofluorescence images taken from hippocampal slices in four groups with different treatments as indicated. ASC/Iba-1/DAPI triple positive cells were spotted in slices treated with Meth and gp120 in combination, but not in slices treated with each alone. Scale bar equals 20 μm. (B) Exemplary band of western blot analysis showing the expression levels of NLRP3, ASC and pro-caspase-1. (C-E) Band densitometry data from 4 independent experiments, normalized with the controls, showed Meth and gp120 in combination (M+g) upregulated the expression levels of ASC ($n = 5$, compared to gp120

alone) and procaspase-1 (n = 8, compared to Meth and gp120 each alone). Pretreatment of slices with caspase-1 inhibitor Ac-YVAD-CMK (10 μM) for 1 h significantly blocked the up-regulatory effects of Meth and gp120 on inflammasome complex expression (M+g+A). LPS (100 ng/ml) was used as a positive control. Data are presented as mean ± SEM and analyzed using one-way ANOVA followed by Tukey's post hoc test. $^{*}P < 0.05$, $^{**}P < 0.01$, $^{***}P < 0.001$ vs. control, $^{\#}P < 0.05$, $^{\#\#}P < 0.01$ vs. Meth+gp120.